Earth and Planetary Science Letters 406 (2014) 93–101

Contents lists available at ScienceDirect

Earth and Planetary Science Letters

www.elsevier.com/locate/epsl

Fault strength evolution during high velocity friction experiments with slip-pulse and constant-velocity loading

Zonghu Liao [a,b], Jefferson C. Chang [b], Ze'ev Reches [b,*]

[a] State Key Laboratory of Petroleum Resources and Prospecting, College of Geosciences, China University of Petroleum, Beijing 102249, China
[b] School of Geology and Geophysics, University of Oklahoma, Norman, OK 73072, United States

ARTICLE INFO

Article history:
Received 31 March 2014
Received in revised form 4 September 2014
Accepted 7 September 2014
Available online 28 September 2014
Editor: P. Shearer

Keywords:
friction strength
fault weakening
slip-pulse
earthquake rupture

ABSTRACT

Seismic analyses show that slip during large earthquakes evolves in a slip-pulse mode that is characterized by abrupt, intense acceleration followed by moderate deceleration. We experimentally analyze the friction evolution under slip-pulse proxy of a large earthquake, and compare it with the evolution at loading modes of constant-velocity and changing-velocity. The experiments were conducted on room-dry, solid granite samples at slip-velocities of 0.0006–1 m/s, and normal stress of 1–11.5 MPa. The analysis demonstrates that (1) the strength evolution and constitutive parameters of the granite fault strongly depend on the loading mode, and (2) the slip-pulse mode is energy efficient relatively to the constant-velocity mode as manifested by faster, more intense weakening and 50–90% lower energy dissipation. The results suggest that the frictional strength determined in slip-pulse experiments, is more relevant to simulations of earthquake rupture than frictional strength determined in constant-velocity experiments. Further, for a finite amount of crustal elastic energy, the efficiency of slip-pulse would amplify earthquake instability.

1. Introduction

Fault rupture during an earthquake occurs by a propagating front that activates numerous patches along the fault zone. The activation of a patch is manifested by its acceleration from a locked state to slipping state during the finite period of the rise time (Fig. 1, left). It is envisioned that the rupture during large earthquakes occur in a slip-pulse style that is characterized by two main features: (1) At any given time during the earthquake, slip occurs along a partial segment of the fault, and slip is not simultaneously active along the entire fault; and (2) Abrupt acceleration followed by moderate deceleration (Heaton, 1990; Zheng and Rice, 1998; Anooshehpoor and Brune, 1999; Tinti et al., 2005; Ampuero and Ben-Zion, 2008; Xu et al., 2012; Noda and Lapusta, 2013; Chang et al., 2012). Earthquake slip-pulse is considered as a variant of the Yoffe function of dynamic brittle fracturing in which the slip velocity theoretically rises by infinite acceleration (in practice, the acceleration is finite as shown by the blue curve in Fig. 1, right a) (Kostrov, 1964; Tinti et al., 2005; Lapusta, 2009; Fukuyama and Mizoguchi, 2010). It is assumed that during a slip-pulse, the fault patch undergoes initial weakening that is followed by healing (red, dashed curve, Fig. 1, right a), and this strength evolution is naturally controlled by both the friction–velocity relations and the rupture loading mode. In spite of its significance, the strength evolution during high-velocity slip-pulse was experimentally analyzed only in two high-velocity studies (Fukuyama and Mizoguchi, 2010; Chang et al., 2012), and without systematic comparison to other slip modes.

To explore this behavior, we conducted a series of high-velocity experiments in which we loaded experimental granite faults by pulse-like source-time function (red curve Fig. 1, right b); for simplicity, we refer to this function as 'slip-pulse'. We then compared these results with those of classical constant-velocity (black curve Fig. 1, right b) and changing-velocity (green curve Fig. 1, right b) experiments. The analysis indicates that (i) the frictional strength evolution of slip-pulse mode is fundamentally different from the equivalent relations of the other slip modes, and (ii) slip-pulse mode dissipates less energy than the constant-velocity mode.

2. Experimental set-up

The experiments were conducted with a high-velocity rotary shear apparatus in the University of Oklahoma (Fig. 2a–c). The set-up was described in the 'Online Methods' sections of Reches and Lockner (2010) and Chang et al. (2012). Each sample is composed of two cylindrical rock blocks, each 101.6 mm in diameter,

* Corresponding author. Tel.: +1 405 321 3157.
E-mail address: Reches@ou.edu (Z. Reches).

http://dx.doi.org/10.1016/j.epsl.2014.09.010
0012-821X/

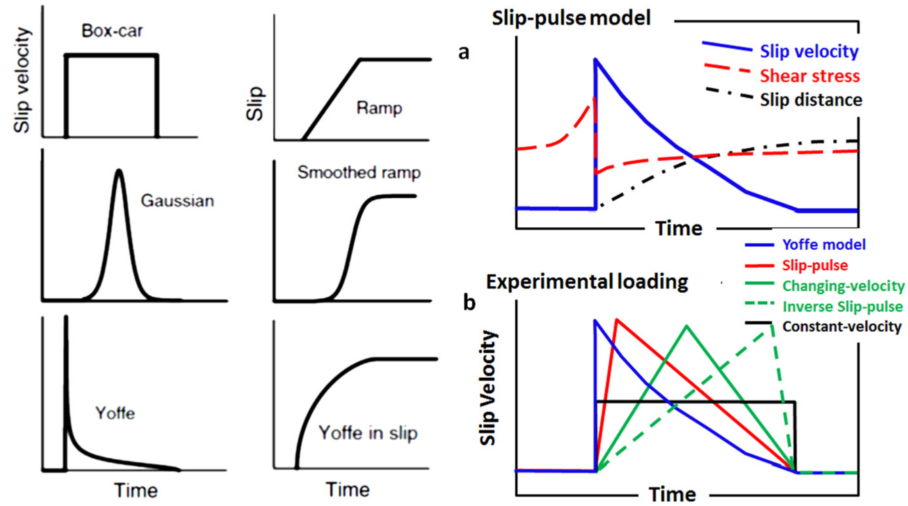

Fig. 1. Conceptual time-history of slip-velocity along a fault patch during a large earthquake. Left. Schematic presentation of a few idealized histories of slip-velocity and slip distance (Tinti et al., 2005). Right a. Schematic presentation of fault patch behavior during slip-pulse loading; arbitrary scales of time slip velocity, shear stress, and slip distance; modified after Heaton (1990). Right b. Schematic presentation of the slip-velocity history used in the present experiments and the idealized Yoffe function (text).

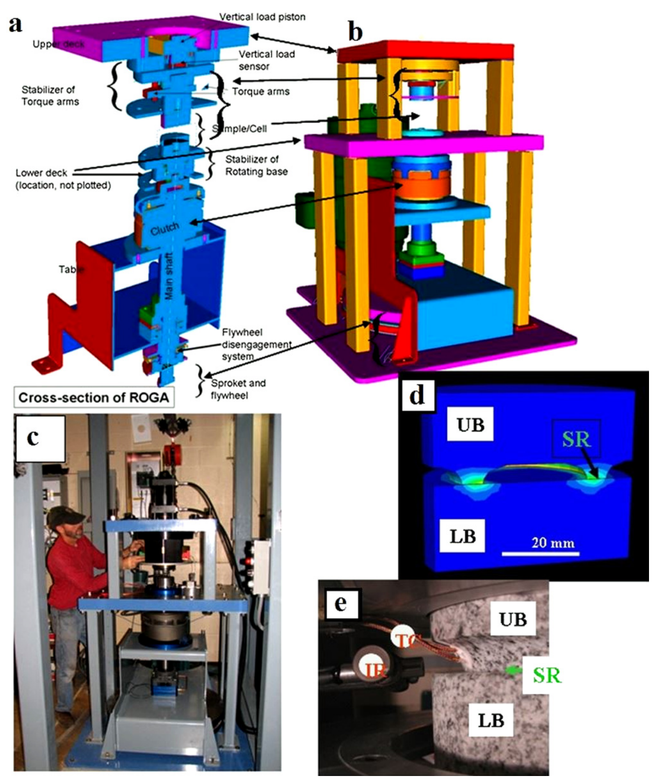

Fig. 2. ROGA, high-velocity shear apparatus (Reches and Lockner, 2010; Chang et al., 2012). a, Generalized cross section displaying main power train components. b, 3D view of the assembled apparatus. c, General view of the system. d and e, Blocks of Sierra White granite used in the present experiments. LB-lower block; UB-upper block; SR-sliding ring; TC-thermocouple wires; IR-infra red sensor. d, A vertical cut-through the blocks in a finite-element model showing model geometry and temperature distribution due to frictional heating. e, Sample blocks assembled in the loading frame; note two thermocouple (TC) wires cemented into the sliding ring.

the upper, stationary block has a raised ring structure, and the blocks were pressed against each other along the raised ring (Fig. 2d, e). The rock blocks are glued by epoxy to aluminum cylindrical holders (Fig. 2d), surface-ground and roughened with 600 grit SiC powder. The normal stress was kept constant during a given experiment. The present experiments were conducted on bare, solid blocks of Radiant Red granite (RRG) that was supplied by ColdSpringGranite, TX. It is composed of quartz (43.6%), albite (19.7%), microcline (22.8%), and biotite (13.9%), in weight percent.

We tested four slip modes of velocity evolution (Fig. 1, right b): (i) slip-pulse mode (red curve) with initial intense acceleration followed by gentle deceleration. This loading mode is regarded as an experimental proxy of the idealized Yoffe function without the infinite initial acceleration (Fukuyama and Mizoguchi, 2010) (blue curve); (ii) the classical constant-velocity mode (black curve) with a selected velocity maintained for a given time period; (iii) changing-velocity mode (green curve) with initial gentle acceleration to peak velocity followed by similar rate of gentle deceleration (Sone and Shimamoto, 2009); and (iv) 'inverse slip-pulse' with initial gentle acceleration followed by intense deceleration after peak velocity (dashed green curve).

3. Experimental observations

3.1. Constant-velocity runs

We conducted 43 experiments on granite samples (RRG) at ambient room conditions (Tables 1, 2). In 35 runs of constant-velocity, the slip-velocity range was $V = 0.0006$ to 0.23 m/s, the normal stresses range was $\sigma_n = 1.0$ MPa to 11.5 MPa, and the total slip distances were up to 4.8 m. The friction coefficient, μ, is presented by the experimental ratio of [shear stress/normal stress].

In a typical constant-velocity experiment, the initial friction coefficient, $\mu_{initial}$, is high and it exponentially drops to a steady-state level (e.g., Fig. 3a). Mizoguchi et al. (2007) showed that the evolution of the friction strength, μ_{CV}, at constant-velocity can be represented by the following relations,

$$\mu_{CV} = \mu_{final} + (\mu_{initial} - \mu_{final}) \exp\left(\frac{\ln(b) \cdot d}{d_c}\right) \quad (1)$$

where μ_{final} is the final friction coefficient, and d_C is the distance over which μ reduces to the fraction b of the total weakening, ($\mu_{initial}$–μ_{final}). Mizoguchi et al. (2007) selected $b = 0.05$ for their experiments with Nojima fault gouge, and considered d_C as the slip weakening distance. In the present analysis, we selected $b = 0.1$ (Fig. 3a). The final friction coefficient was calculated for the final 0.1 m of slip distance, and it is considered as a proxy of the steady-state friction, μ_{steady}.